

# Realization of the field-free Josephson diode

Heng Wu<sup>1,2,4\*</sup>, Yaojia Wang<sup>2,4</sup>, Pranava K. Sivakumar<sup>2</sup>, Chris Pasco<sup>3</sup>, Stuart S. P. Parkin<sup>2</sup>, Yu-Jia Zeng<sup>1</sup>, Tyrel McQueen<sup>3</sup>, Mazhar N. Ali<sup>2\*</sup>

<sup>1</sup>College of Physics and Optoelectronic Engineering, Shenzhen University, Shenzhen 518060, China

<sup>2</sup>Max Planck Institute of Microstructure Physics, Halle, Saxony-Anhalt, 06108, Germany

<sup>3</sup>Johns Hopkins University, Baltimore, Maryland 21218, USA

<sup>4</sup>These authors contributed equally.

\*e-mail: [wuhenggcc@gmail.com](mailto:wuhenggcc@gmail.com), [maz@berkeley.edu](mailto:maz@berkeley.edu)

Abstract:

**The superconducting analog to the semiconducting diode, the Josephson diode, has long been sought, with multiple avenues to realization proposed by theorists<sup>1-3</sup>. Exhibiting magnetic-field free, single directional superconductivity with Josephson coupling of the supercurrent across a tunnel barrier, it would serve as the building-block for next-generation superconducting circuit technology. Here we realized the field-free Josephson diode using an inversion symmetry breaking heterostructure of NbSe<sub>2</sub>/Nb<sub>3</sub>Br<sub>8</sub>/NbSe<sub>2</sub>. We demonstrate, for the first time without magnetic field, the junction can be superconducting in one direction while normal in the opposite direction. Based on that, half-wave rectification of a square-wave excitation was achieved with low switching current density ( $\sim 2.2 \times 10^2$  A/cm<sup>2</sup>), high rectification ratio ( $\sim 10^4$ ) and high robustness (at least  $10^4$  cycles). We also demonstrate symmetric  $\Delta I_c$  (the difference between positive and negative critical currents) behavior with field and the expected Fraunhofer current phase relation of a Josephson junction. This realization raises fundamental questions about the Josephson effect through an insulator when breaking symmetry, and opens the door to ultralow power, high speed, superconducting circuits for logic and signal modulation.**

Nonreciprocity in charge transport describes the electric field direction dependent behavior of electrical current i.e. the current generated by a positive voltage is asymmetric with that generated by a negative voltage. Nonreciprocal behavior is the basis for numerous important electronic devices such as diodes, rectifiers, AC/DC converters, photodetectors, transistors and more<sup>4-6</sup>. A well-known example of a nonreciprocal device is the p-n junction, formed by the interface of a p-doped and n-doped semiconductor, which exhibits an asymmetric current-voltage characteristic (IVC) and is widely used in various semiconducting technologies including logic and computation<sup>7</sup>. However energy dissipation in these devices cannot be avoided due to both resistive “on” and “off” states, and the power consumption and heat dissipation of exascale computing remains a highly challenging problem<sup>8</sup>. Hence superconducting computing using Josephson junctions (JJ) has been an important research direction for several decades, taking advantage of up to a 1000 times reduction in power as well as ultrafast switching speeds with operating frequencies approaching the THz regime<sup>9-12</sup>. However unlike the p-n junction, JJs are known to exhibit symmetric IVC at zero magnetic field where the response of the junction under forward bias is the same as with reverse bias.

Recently, nonreciprocal superconductivity, has been seen due to magnetochiral anisotropy in noncentrosymmetric superlattices<sup>13</sup>, superconductors<sup>14,15</sup>, heterostructures<sup>16,17</sup> and topological materials<sup>18,19</sup>. Magnetochiral anisotropy<sup>20-23</sup> requires simultaneous breaking of inversion symmetry ( $\mathcal{P}$ ) and time reversal symmetry ( $\mathcal{T}$ ). With sufficient magnetic field strength, it was shown that the critical current to destroy the superconducting state in one direction can be different from that in the other direction<sup>13</sup>. Also, nonreciprocal superconductivity was seen through an alternative mechanism in planar JJs of Nb/WTe<sub>2</sub>/Nb, where a lack of inversion symmetry in WTe<sub>2</sub> allowed for differing Fermi velocities of its edge states and resulted in an asymmetric Josephson effect under magnetic field<sup>3,18</sup>. As yet, nonreciprocal superconductivity has never been observed in either bulk superconductors or JJs without an applied magnetic field.

However, in principle, nonreciprocal superconductivity is allowed to appear in JJs that are only  $\mathcal{P}$ -breaking (while preserving  $\mathcal{T}$ ), analogous to the situation in p-n junctions. Misaki et al recently proposed that in  $\mathcal{P}$ -breaking JJs with a large capacitance, the accumulation of charge on opposite sides of the junction will be different, leading to a charging energy difference and correspondingly nonreciprocal behavior<sup>1</sup>. Alternatively, Hu *et al.* proposed that in JJs formed by mating a p-doped and an n-doped superconductor, the interface would create a Mott-insulating region which would also result in an asymmetric IVC<sup>2</sup>. These studies imply that it is possible to fabricate a “Josephson diode”, allowing supercurrent in one direction but normal current in the other direction in the absence of magnetic field, which is highly desired for superconducting electronics, particularly superconducting computing approaches like rapid single flux quantum (RSFQ) and latch logic<sup>9,24</sup>.

Here we report field-free supercurrent rectification in a Josephson diode based on a  $\mathcal{P}$ -breaking heterostructure of two NbSe<sub>2</sub> flakes separated by the insulator Nb<sub>3</sub>Br<sub>8</sub>. An asymmetric IVC is seen at zero magnetic field revealing the Josephson diode behavior. Half-wave rectification of a superconducting square-wave excitation is demonstrated with large on/off ratio, ultralow switching current density, correspondingly low switching power, and highly stable performance. The field-free Josephson diode effect lies in the asymmetric tunneling of the supercurrent across the tunnel barrier, and the  $\mathcal{P}$ -breaking of the junction is further confirmed by antisymmetric second harmonic peaks. The effect shown here can be extended to a variety of material systems and architectures for the advancement of future superconducting electronics and quantum devices.

We fabricated vertical JJs in a 2D heterostructure form by stacking thin flakes of NbSe<sub>2</sub> on either side of a Nb<sub>3</sub>Br<sub>8</sub> flake as shown in Fig. 1a. This vertical junction architecture is used to facilitate tunneling of the supercurrent through the insulating barrier. As a heavier version of insulating Nb<sub>3</sub>Cl<sub>8</sub><sup>25-29</sup>, Nb<sub>3</sub>Br<sub>8</sub> is a 2D van der Waals material that crystallizes in the  $R\bar{3}m$  space group at low temperature and its unit cell is comprised of 6 layers of Nb-Br edge-sharing octahedra. Inversion symmetry broken flakes can be obtained by exfoliation of an odd number of layers. Also, a singlet magnetic ground state has been observed in this structure<sup>25</sup>. Thus Nb<sub>3</sub>Br<sub>8</sub> is an ideal tunnel barrier for creating a van der Waals stacked JJ with exotic behavior; it is highly exfoliatable, has a

moderate band gap and can intrinsically break inversion symmetry (which can further be guaranteed by having different interfaces with the top and bottom NbSe<sub>2</sub> layers). Our NbSe<sub>2</sub>/Nb<sub>3</sub>Br<sub>8</sub>/NbSe<sub>2</sub> heterostructures were fabricated by the dry transfer method<sup>30</sup> (see Methods) and capped by a top h-BN layer to avoid degradation, as a typical device in the inset of Fig. 1b shows. Here thick NbSe<sub>2</sub> flakes with thickness about 28 - 37 nm are used as superconducting electrodes, rotated by arbitrary angles with respect to each other, and a thin flake of Nb<sub>3</sub>Br<sub>8</sub> with thickness of 2.3 nm (3 layers) is used as the tunnel barrier.

While cooling the junction to 20 mK in zero field, a sudden drop to zero resistance at  $T_c = 6.6$  K is observed, as shown in Fig. S1a. Figure 1b investigates the voltage vs. current ( $V$ - $I$ ) behavior, measured by sweeping the DC current at 20 mK (see  $V$ - $I$  curves at different temperatures in Fig. S1b). We emphasize that measurement of  $V$ - $I$  curves contain four branches; sweeping the current from zero to a positive value (0-p), from a positive value back to zero (p-0), from zero to a negative value (0-n) and from a negative value back to zero (n-0). Additionally, these four branches can be done in the above order (defined as the positive sweep), or in reverse order, 0-n, n-0, 0-p, and p-0 (defined as the negative sweep). Fig. 1b shows two  $V$ - $I$  curves; the positive sweep and the negative sweep. Note that the properties measured here all come from the JJ itself as the maximum current applied here is much smaller than the critical current of thick NbSe<sub>2</sub> (few milliamps)<sup>31</sup>. Both  $V$ - $I$  curves exhibit hysteresis, as expected, arising from the capacitance of the JJ resulting in different critical currents when breaking superconductivity ( $I_c$ ) compared with returning to superconductivity ( $I_r$ )<sup>1</sup>. Importantly, the two curves lie precisely on top of each other meaning that the positive versus negative sweep order does not affect the  $V$ - $I$  response. However, the  $I_c$  and  $I_r$  in the positive current regime (labelled  $I_{c+}$  and  $I_{r+}$ ) can be compared with  $I_c$  and  $I_r$  in the negative current regime (labelled  $I_{c-}$  and  $I_{r-}$ ). For reciprocal transport, as is expected for a conventional JJ without magnetic field, there should be no difference between  $I_{c+}$  vs.  $|I_{c-}|$  or  $I_{r+}$  vs.  $|I_{r-}|$ .

Figure 1c shows the absolute values of  $I_{c+}$  and  $I_{r+}$  as well as  $I_{c-}$  and  $I_{r-}$  of the positive sweep. Immediately evident is that  $I_{c+}$  and  $I_{r+}$  are not equal to their negative current counterparts, although  $V_{c+} = |V_{c-}|$  (the voltage at the critical current), with a  $\Delta I_c \sim 0.5$   $\mu$ A and a smaller  $\Delta I_r \sim 0.1$   $\mu$ A, indicating the nonreciprocal  $V$ - $I$  response in our JJ. It is important to note that these differences are intrinsic properties of the JJ rather than an extrinsic Joule heating effect (see discussion in Methods). The different absolute values of  $I_{c+}$  and  $I_{c-}$  combined with the sharp superconducting transition imply that when the applied current is in between  $I_{c+}$  and  $|I_{c-}|$ , the junction would exhibit superconducting behavior with a negative current but normal conducting behavior with a positive current.

Based on this idea, we demonstrated half-wave rectification at zero field, as shown in Fig 2a. Due to the  $I_{c+}$  and  $|I_{c-}|$  being 7.61  $\mu$ A and 8.14  $\mu$ A, respectively, we applied a square-wave excitation (Fig 2a top panel) with an amplitude of 7.9  $\mu$ A at a frequency of 0.1 Hz. As shown in the bottom panel of Fig 2a, the junction remains in the superconducting state with the negative current (purple area) while switching to the normal state during the positive current (white area). The measured voltage in the superconducting state is smaller than  $4 \times 10^{-7}$  V (the lowest detectable limit of our

instrument), while the normal state junction voltage is 1.6 mV, meaning the diode rectification ratio demonstrated here is at least  $\sim 10^4$ . In addition, the switching current density and switching power are  $2.2 \times 10^2$  A/cm<sup>2</sup> and 12.3 nW, respectively, which are 2 and 4 orders of magnitude smaller than in the bulk superconducting diode<sup>13</sup>.

We further probed the durability of the Josephson diode and robustness of half-wave rectification, as shown in Fig. 2b by conducting 10,000 continuous cycles with an applied square-wave excitation with an amplitude of 7.9  $\mu$ A at 0.5 Hz and zero field. We note that the “on” and “off” state voltages stayed constant during the 10,000 cycles, and the device remains stable after that, indicating the high stability of the Josephson diode. Importantly, the Josephson diode effect is not just an ultralow temperature property; according to the asymmetric  $V$ - $I$  curves observed at 0.9 K and 3.86 K (see Fig. S2), an ideal half-wave rectification was also realized at 0.9 K while the half-wave rectification at 3.86 K had some punch-through error likely due to the thermal fluctuation as shown in Fig. S2b and S2d, respectively. In addition, the large hysteresis at ultralow temperatures indicates the junction is in the strongly underdamped regime. Therefore at 20 mK, the estimated Stewart-McCumber parameter ( $\beta_c \approx \left(\frac{4I_c}{\pi I_T}\right)^2$ ) is 21 and the junction capacitance calculated by equation  $\beta_c = \frac{2e}{\hbar} I_c R_N^2 C$  (where  $R_N$  is normal state resistance of junction) is  $2.0 \times 10^{-14}$  F, corresponding with specific capacitance ( $C/A$ ,  $A \approx 3.68 \mu\text{m}^2$ ) of  $0.54 \mu\text{F}/\text{cm}^2$  (ref. <sup>32,33</sup>). However, by 3.86 K, the p-0 (n-0) almost coincides with the 0-p (0-n) branch, indicating the junction changed to the overdamped regime, allowing possible operation frequencies on the order of the superconducting switching speed (THz)<sup>34</sup>.

In order to further confirm the field-free behavior of the Josephson diode effect, we performed  $V$ - $I$  curves containing 0-p and 0-n branches with applying an in-plane magnetic field (inset of Fig. 3a) from 40 mT to -40 mT (sweep down) with a step of 0.5 mT. As before, the  $I_{c+}$  and  $|I_{c-}|$  was extracted and plotted in Fig. 3a ( $V$ - $I$  curves with magnetic field were shown in Fig. S3). Both  $I_{c+}$  and  $|I_{c-}|$  decrease with the increasing magnetic field, and almost reach 0 by 40 mT, which reflects the magnetic field dependent current phase relation of a JJ which will be addressed in Fig. 4. Below 35 mT,  $\Delta I_c$  ( $\Delta I_c = |I_{c-}| - I_{c+}$ ) emerges, as the  $I_{c+}$  increases less rapidly than  $|I_{c-}|$  as the magnetic field goes to 0. Note that  $|I_{c-}|$  stays larger than  $I_{c+}$  regardless of the direction of the magnetic field. Fig. 3b shows the  $\Delta I_c$  plotted as a function of magnetic field; the  $\Delta I_c$  is sustained at zero field and its magnitude is independent of field in the low-field region. The Fig. 3b inset shows how  $\Delta I_c$  varies with decreasing  $|I_{c-}|$  and  $|I_{c-}|$  can be up to 25% larger than  $I_{c+}$ . The field dependent  $\Delta I_c$  behavior here differs from that in the magnetochiral anisotropy induced superconducting diode effect, where the  $\Delta I_c$  exhibits an antisymmetric field dependent behavior due to the magnetochiral anisotropy<sup>13</sup>. Therefore, diodic behavior based on magnetochiral anisotropy must necessarily shut off at zero magnetic field and vary quickly near zero field. Also, in a bulk superconductor with magnetochiral anisotropy,  $\Delta I_c$  vs  $B$  is sweep direction dependent, flipping sign<sup>13</sup>, while in the field-free Josephson diode demonstrated here,  $\Delta I_c$  vs  $B$  shows no difference with sweep direction (see Fig. S4).

To prove Josephson coupling of the electrodes, the  $dV/dI$  mapping as a function of bias current and magnetic field was measured and is shown in Fig. 4a. As expected, the characteristic single slit Fraunhofer pattern from the Josephson effect is observed. The critical current of the JJ decreases rapidly with increasing magnetic field, consistent with the  $I_c$  decreasing in Fig. 3a. To further investigate the relationship between the observed nonreciprocal behavior and symmetry breaking conditions, the field dependent first and second harmonic resistances were measured with an AC current with an amplitude of 5  $\mu\text{A}$  and frequency of 7.919 Hz, as shown in Fig. 4b. The sharp drop of the first harmonic resistance in  $\sim \pm 30$  mT shows the onset of superconductivity while the two antisymmetric peaks appear in the second harmonic resistance at the same fields indicating that inversion symmetry in the junction must be broken<sup>13,14,35</sup>. There are two reasons for this junction being  $\mathcal{P}$ -breaking. First, is the geometry of the vertical junction where the top and bottom NbSe<sub>2</sub> electrodes have different thickness and alignment (rotation) with the Nb<sub>3</sub>Br<sub>8</sub> layer. Second, the thin Nb<sub>3</sub>Br<sub>8</sub> flakes are 3 layers, which intrinsically lack inversion symmetry.

Fundamentally, to obtain a  $\Delta I_c$  and  $\Delta I_r$ , an asymmetric  $V$ - $I$  curve is required i.e. the  $I_+$  behavior needs to be distinct from the  $I_-$  behavior. From the phenomenological RCSJ model of a JJ (Resistively and Capacitively Shunted Junction), the total current through the junction  $I$  is determined by  $I = I_F + I_C + I_R + I_J$ , where  $I_F$  is the fluctuation current of the noise channel,  $I_C$  is the current of the capacitive channel,  $I_R$  is the additional resistive channel arising from finite temperature quasiparticle excitation, and  $I_J$  is the Josephson current. In DC measurement, the thermal noise current ( $I_T$ ) dominates the fluctuation current, which can be calculated according to equation  $I_T = (2e/\hbar)k_B T$  (ref. <sup>32</sup>), where  $\hbar$  is reduced Planck constant,  $k_B$  is Boltzmann constant,  $e$  is elementary charge, and  $T$  is the temperature. At 20 mK,  $I_T$  is about 0.8 nA, far less than  $\Delta I_c$ , and so will be disregarded as a cause of the  $V$ - $I$  asymmetry. In principle, the other three components could have asymmetric  $V$ - $I$  responses if inversion/time reversal symmetry is broken. Below we examine each of those possibilities in the context of our JJ.

Regarding the capacitive channel, as mentioned earlier, Misaki *et al.*<sup>1</sup> proposed that in an inversion symmetry broken JJ, an asymmetric charging energy of capacitance can lead to a  $\Delta I_r$ , without an applied magnetic field, which was observed in our JJ device (Fig. 1c). However, this model did not include an expectation of a  $\Delta I_c$ , which is the main requirement for realizing half-wave rectification. Since  $I_r$  corresponds with the return to the superconducting state, applying a square-wave current excitation with an amplitude of  $I_{r+} + \Delta I_r/2$ , for example, would not result in rectification as both ends of the wave lie within the superconducting regime.

Considering the additional resistive channel ( $I_R = V/R_N$ ) from quasiparticle excitations, its contribution to the diodic effect would stem from asymmetry in  $R_N$  and be significant if the resistance in the superconducting state was not 0. However, since the voltage in superconducting state is 0 in our device, the contribution of  $I_R$  to the critical current can be neglected. The critical current through the JJ will be governed by the Josephson current  $I_J$ , ( $I_J = I_c \sin \varphi$ ,  $I_c = V_c/R_N$  and  $\varphi$  is

phase difference of two superconductors). Since  $\Delta I_c$  is suppressed with applied field and  $I_{c+}$  and  $I_{c-}$  are symmetric with applied field, magnetochiral anisotropy can be ruled out as the driving mechanism here. Also a thick NbSe<sub>2</sub> is not a  $\mathcal{T}$ -breaking superconductor nor is Nb<sub>3</sub>Br<sub>8</sub> ferromagnetic at low temperature<sup>25</sup>. Therefore  $\Delta I_c$  should be induced by asymmetric Josephson tunnelling at zero field in our junction.

Recently, Kitamura et al. discussed non-reciprocal Landau-Zener tunneling in  $\mathcal{P}$ -breaking materials, explaining that the effect in the normal state is a product of direction dependent modulation of the electron tunneling probability across a tunnel barrier due to a shift in wave-packet position<sup>36</sup>. Altering the tunneling probability replicates a diodic response through wavefunction modulation rather than an energetic change like a p-n diode. Although the ingredients for this picture are also present in this Josephson diode, the tunneling mechanics would be different; the tunneling supercurrent should lie in the Andreev tunneling regime. Alternatively, Hu et al proposed a Josephson diode based on an interface of p and n-doped superconductors that implicitly breaks inversion symmetry and forms a Mott insulating region<sup>2</sup>. Like a p-n semiconducting diode with a built in electric field, this region can be suppressed with voltage in one direction and elongated with the other direction, resulting in diodic behavior. Our JJ architecture is also  $\mathcal{P}$ -breaking, however it is unclear whether the different interfaces or the barrier itself lead to direction dependent modulation in analogy to the Hu et al. proposal. At this time it is unknown if Nb<sub>3</sub>Br<sub>8</sub> can host an internal polarization in the odd layer limit (as in this study) where it breaks inversion symmetry. Further theoretical examination of inversion symmetry breaking JJ's is necessary.

In summary, we have realized, for the first time, a Josephson diode with magnetic field free, unidirectional superconductivity and Josephson coupling of supercurrent across the tunnel barrier. Using a heterostructure of 2D flakes of NbSe<sub>2</sub> and Nb<sub>3</sub>Br<sub>8</sub>, we demonstrated that  $I_{c-}$  can be up to 25% larger than  $I_{c+}$  as well as durable half-wave rectification with rectification ratios of at least  $10^4$ , with a switching current density as low as  $2.2 \times 10^2$  A/cm<sup>2</sup>. Optimization of this Josephson diode architecture through tuning the thickness or type of the barrier can result in more ideal diodic behavior. However, creating further Josephson diode architectures like demonstrated here can uncover emergent phenomena when combining multiple traits together. Future work combining symmetry breaking materials possessing properties such as topological states, ferroelectricity, magnetoelectricity, noncollinear magnetism, multiferroicity, etc. with superconducting electrodes will allow realization of a plethora of novel Josephson phenomena. In addition, these quantum materials allow for tuning and optimization of Josephson diode properties for RSFQ devices, Qubits, latching devices, and other superconducting circuits both in planar and vertical architectures. Thus the opportunities for creating superconducting electronics utilizing quantum materials are vast and just beginning.

## References

- 1 Kou Misaki & Nagaosa, N. Theory of nonreciprocal Josephson effect. <https://arxiv.org/abs/2002.06458> (2020).
- 2 Hu, J., Wu, C. & Dai, X. Proposed design of a Josephson diode. *Phys. Rev. Lett.* **99**, 067004 (2007).
- 3 Chen, C.-Z. et al. Asymmetric Josephson effect in inversion symmetry breaking topological materials. *Phys. Rev. B* **98**, 075430 (2018).
- 4 Tokura, Y. & Nagaosa, N. Nonreciprocal responses from non-centrosymmetric quantum materials. *Nat. Commun.* **9**, 3740 (2018).
- 5 Rikken, G. L. J. A. & Raupach, E. Observation of magneto-chiral dichroism. *Nature* **390**, 493-494 (1997).
- 6 Ideue, T. et al. Bulk rectification effect in a polar semiconductor. *Nat. Phys.* **13**, 578-583 (2017).
- 7 Sze, S. M. & Lee, M.-K. *Semiconductor Devices: Physics and Technology*, 3rd Edition (Wiley, 2012).
- 8 Bergman, K. et al. Exascale computing study: Technology challenges in achieving exascale systems. *tech. report TR-2008-13, Dept. of Computer Science and Eng., Univ. of Notre Dame*, 2008 (2008).
- 9 Clarke, J. & Wilhelm, F. K. Superconducting quantum bits. *Nature* **453**, 1031-1042 (2008).
- 10 Devoret, M. H. & Schoelkopf, R. J. Superconducting circuits for quantum information: An outlook. *Science* **339**, 1169 (2013).
- 11 Walsh, E. D. et al. Josephson-junction infrared single-photon detector. <https://arxiv.org/abs/2011.02624> (2020).
- 12 Lee, G.-H. et al. Graphene-based Josephson junction microwave bolometer. *Nature* **586**, 42-46 (2020).
- 13 Ando, F. et al. Observation of superconducting diode effect. *Nature* **584**, 373-376 (2020).
- 14 Zhang, E. et al. Nonreciprocal superconducting NbSe<sub>2</sub> antenna. *Nat. Commun.* **11**, 5634 (2020).
- 15 Neupane, M. et al. Observation of the spin-polarized surface state in a noncentrosymmetric superconductor BiPd. *Nat. Commun.* **7**, 13315 (2016).
- 16 Baumgartner, C. et al. A Josephson junction supercurrent diode. <https://arxiv.org/abs/2103.06984> (2021).
- 17 Yasuda, K. et al. Nonreciprocal charge transport at topological insulator/superconductor interface. *Nat. Commun.* **10**, 2734 (2019).
- 18 Kononov, A. et al. One-dimensional edge transport in few-layer WTe<sub>2</sub>. *Nano Lett.* **20**, 4228-4233 (2020).
- 19 Wang, W. et al. Evidence for an edge supercurrent in the Weyl superconductor MoTe<sub>2</sub>. *Science* **368**, 534-537 (2020).
- 20 Wang, Y. et al. Gigantic magnetochiral anisotropy in the topological semimetal ZrTe<sub>5</sub>. <https://arxiv.org/abs/2011.03329> (2021).
- 21 Rikken, G. L. J. A., Fölling, J. & Wyder, P. Electrical magnetochiral anisotropy. *Phys. Rev. Lett.* **87**, 236602 (2001).
- 22 Rikken, G. L. J. A. & Wyder, P. Magnetoelectric anisotropy in diffusive transport. *Phys. Rev. Lett.* **94**, 016601 (2005).
- 23 Ideue, T., Koshikawa, S., Namiki, H., Sasagawa, T. & Iwasa, Y. Giant nonreciprocal

- magnetotransport in bulk trigonal superconductor PbTaSe<sub>2</sub>. *Phys. Rev. Research* **2**, 042046(R) (2020).
- 24 Likharev, K. K. & Semenov, V. K. RSFQ logic/memory family: a new Josephson-junction technology for sub-terahertz-clock-frequency digital systems. *IEEE Trans. Appl. Supercond.* **1**, 3-28 (1991).
  - 25 Pasco, C. M., El Baggari, I., Bianco, E., Kourkoutis, L. F. & McQueen, T. M. Tunable magnetic transition to a singlet ground state in a 2D van der Waals layered trimerized Kagome magnet. *ACS Nano* **13**, 9457-9463 (2019).
  - 26 Haraguchi, Y. et al. Magnetic-nonmagnetic phase transition with interlayer charge disproportionation of Nb<sub>3</sub> trimers in the cluster compound Nb<sub>3</sub>Cl<sub>8</sub>. *Inorg. Chem.* **56**, 3483-3488 (2017).
  - 27 Sheckelton, J. P., Plumb, K. W., Trump, B. A., Broholm, C. L. & McQueen, T. M. Rearrangement of van der Waals stacking and formation of a singlet state at T = 90 K in a cluster magnet. *Inorg. Chem. Front.* **4**, 481-490 (2017).
  - 28 Yoon, J. et al. Anomalous thickness-dependent electrical conductivity in van der Waals layered transition metal halide, Nb<sub>3</sub>Cl<sub>8</sub>. *J. Phys.: Condens. Matter* **32**, 304004 (2020).
  - 29 Jiang, J. et al. Exploration of new ferromagnetic, semiconducting and biocompatible Nb<sub>3</sub>X<sub>8</sub> (X = Cl, Br or I) monolayers with considerable visible and infrared light absorption. *Nanoscale* **9**, 2992-3001 (2017).
  - 30 Castellanos-Gomez, A. et al. Deterministic transfer of two-dimensional materials by all-dry viscoelastic stamping. *2D Mater.* **1**, 011002 (2014).
  - 31 Xi, X. et al. Ising pairing in superconducting NbSe<sub>2</sub> atomic layers. *Nat. Phys.* **12**, 139-143 (2015).
  - 32 Kikharev, K. K. *Dynamics of Josephson junctions and circuits* (Gordon and Breach Science Publishers, 1986).
  - 33 Likharev, K. K. Superconducting weak links. *Rev. Mod. Phys.* **51**, 101-159 (1979).
  - 34 Kleiner, R., Koelle, D., Ludwig, F. & Clarke, J. Superconducting quantum interference devices: State of the art and applications. *Proc. IEEE* **92**, 1534-1548 (2004).
  - 35 Wakatsuki, R. et al. Nonreciprocal charge transport in noncentrosymmetric superconductors. *Sci. Adv.* **3**, e1602390 (2017).
  - 36 Kitamura, S., Nagaosa, N. & Morimoto, T. Nonreciprocal Landau–Zener tunneling. *Commun. Phys.* **3** (2020).



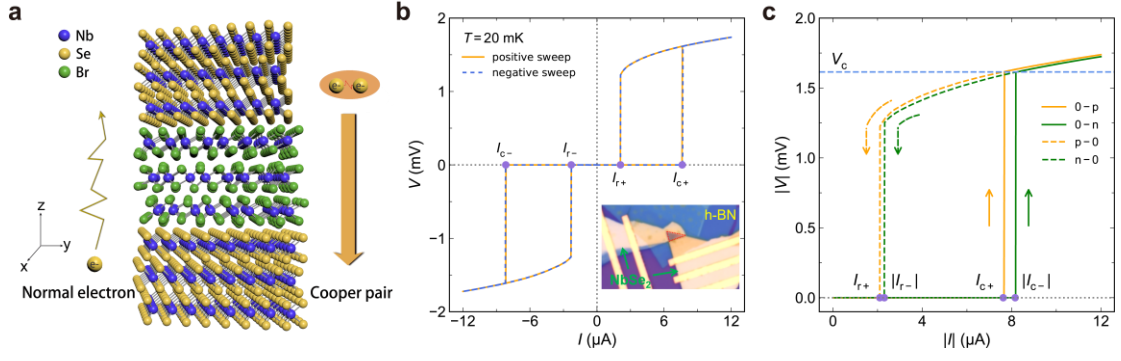


**Fig. 1 | Schematic and superconductivity of the Josephson diode at zero field.** **a**, Schematic of Josephson diode in a vertical Josephson Junction architecture, consisting of an  $\text{NbSe}_2/\text{Nb}_3\text{Br}_8/\text{NbSe}_2$  sandwich. The junction lacks inversion symmetry along the  $z$ -direction, and can exhibit normal conduction in one direction but superconductivity in the other (cooper pair conduction). **b**, Voltage vs current curves measured by sweeping positive (orange solid line) and sweeping negative (blue dashed line), as defined in the main text. Inset shows a typical device architecture, the red triangle outlines the Josephson junction geometry created by the overlapping flakes. **c**, Voltage vs current curves with positive sweep; the orange solid and dashed lines correspond with the 0-p and p-0 branches, respectively, while the green solid and dashed lines correspond with the 0-n and n-0 branches, respectively. The purple dots mark the position of  $I_{c+}$ ,  $|I_{c-}|$ ,  $I_{r+}$  and  $|I_{r-}|$  and the blue dashed line shows the  $V_c$ .

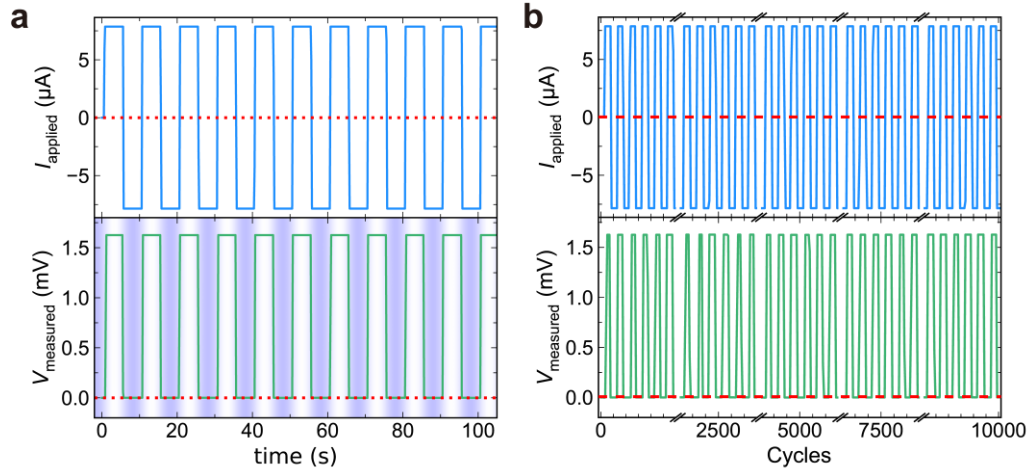


**Fig. 2 | Half-wave rectification and durability test of the Josephson diode at 20 mK and zero-field.** **a**, Top panel is the applied square-wave excitation with an amplitude of  $7.9 \mu\text{A}$  (in between  $I_{c+}$  and  $|I_{c-}|$ ) and frequency of 0.1 Hz. The bottom panel is the coincidentally measured junction voltage. The purple shaded region denotes the superconducting state where the voltage is 0 during negative current bias and the white region denotes the normal state where the voltage is  $V_c$  during positive current bias. The red dotted line is the zero line. **b**, The top panel is the applied square-wave excitation with an amplitude of  $7.9 \mu\text{A}$  and frequency of 0.5 Hz over 10,000 cycles. The bottom panel is the coincidentally measured junction voltage over those cycles, showing no degradation in the response. The red dashed lines are zero lines.

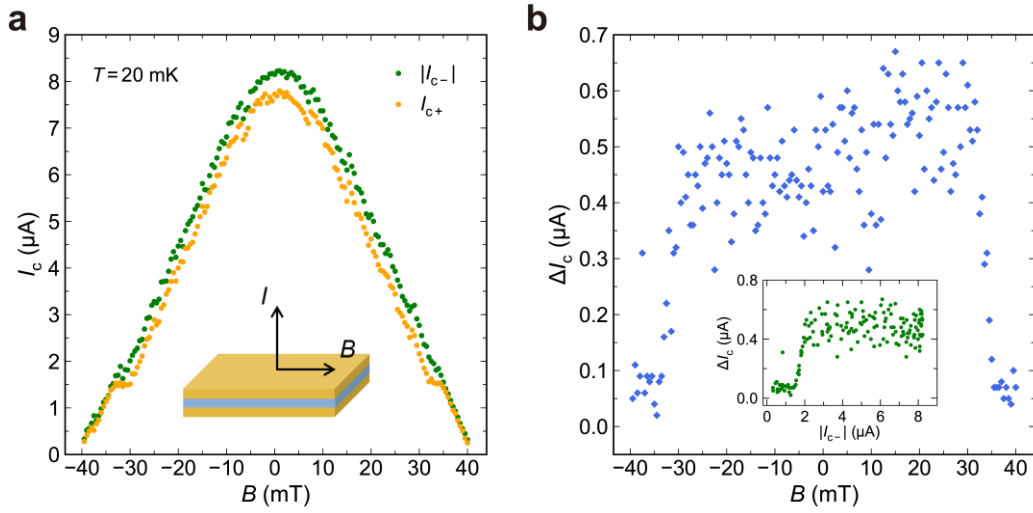


**Fig. 3 | Magnetic field dependence of  $I_c$  and  $\Delta I_c$ .** **a**,  $I_{c+}$  (orange dots) and  $|I_{c-}|$  (green dots) obtained from the 0-p and 0-n branches of the positive sweep as a function of applied magnetic field. The magnetic field was swept from positive to negative. The diode effect “turns off” by  $\pm 35$  mT. Inset is a schematic of the measurement geometry, the orange and blue layers represent  $\text{NbSe}_2$  and  $\text{Nb}_3\text{Br}_8$ , respectively. **b**,  $\Delta I_c$  as a function of magnetic field.  $\Delta I_c$  is roughly field invariant until 35 mT with the diode behavior robust in zero field. Inset shows  $\Delta I_c$  as a function of  $|I_{c-}|$  from modulation of magnetic field with the diode effect “turning off” below  $2.1 \mu\text{A}$ .

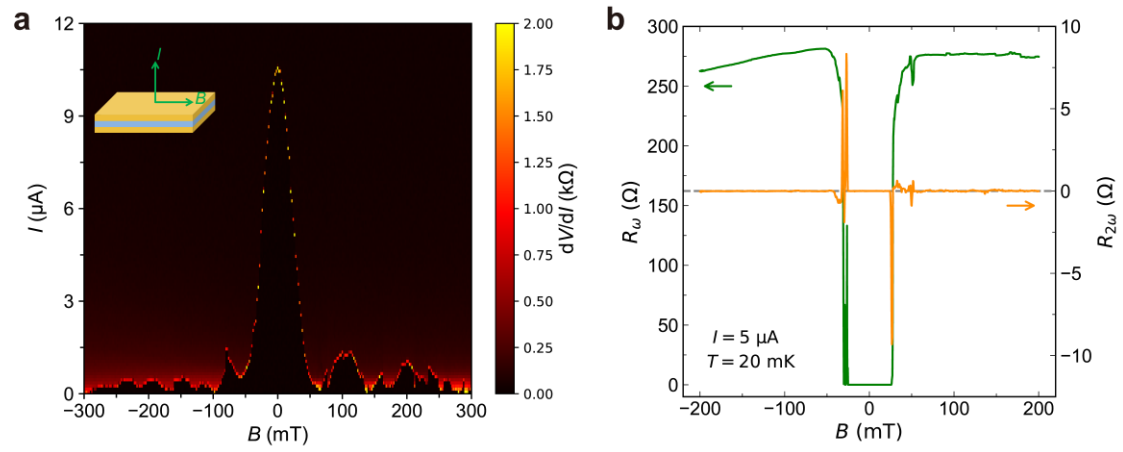


**Fig. 4 | Critical current map and second harmonic resistance of the Josephson diode. a,** Color map of  $dV/dI$  as a function of external magnetic field and applied current, showing the single slit Fraunhofer pattern from the Josephson effect of a Josephson junction. **b,** First (green line) and second harmonic (orange line) resistances measured by applying AC current of  $5 \mu\text{A}$  at  $20 \text{ mK}$ . The antisymmetric peaks in the second harmonic correspond with the critical field, showcasing the nonreciprocal nature of the superconductivity.

## Methods

### Synthesis of Nb<sub>3</sub>Br<sub>8</sub> crystal

Nb<sub>3</sub>Br<sub>8</sub> crystals used in this work were grown through chemical vapor transport. Stoichiometric mixtures of niobium powder (Alfa, 99.99%), and NbBr<sub>5</sub> (Strem, 99.9%) with a total mass of 1.5 g were ground together and added to a 14×16 mm diameter fused silica tube in a glovebox and handled using standard air free techniques. 20 mg of NH<sub>4</sub>Br was included as a transport agent. The tubes were then sealed air free at a length of approximately 30 cm, about 5 cm longer than the first two zones of a three-zone furnace. A three-zone furnace was used with a temperature gradient of 840°C, 785°C and 795°C with all but the last few centimeters of the tube between the first two zones. This discouraged the formation of large intergrown clumps of crystals at the end of the tube. The furnace was held at temperature for 3-5 days before being cooled to room temperature over 7 hours.

### Fabrications of the Josephson junction device.

We fabricated the NbSe<sub>2</sub>/Nb<sub>3</sub>Br<sub>8</sub>/NbSe<sub>2</sub> Josephson junction in glove box with inert environment to avoid oxidation and decay. The bottom NbSe<sub>2</sub> flake was directly exfoliated from a NbSe<sub>2</sub> single crystal (HQ graphene) to a SiO<sub>2</sub>/Si wafer, then Nb<sub>3</sub>Br<sub>8</sub> thin film and top NbSe<sub>2</sub> flake were exfoliated and successively transferred layer by layer by using PDMS assistant dry transfer method<sup>30</sup>. A h-BN (HQ graphene) layer was finally transferred on the top to protect the JJ from degradation in the atmosphere. Then Ti (3 nm)/Au (50 nm) electrodes were deposited on top and bottom NbSe<sub>2</sub> flakes for transport measurement.

### Transport measurements

The transport properties of JJ device were measured in a BlueFors dilution refrigerator with a base temperature of 20 mK. A Keithley 6221 AC/DC Current Source Meter was used to inject both DC current and square-wave excitation, and the DC voltage was measured with a Keithley 2182a Nanovoltmeter. The AC measurements were performed by injecting AC current with frequency of  $\omega$  (7.919 Hz) using Zurich MFLI, and the second-harmonic signals were obtained from the out-of-phase  $2\omega$  component of the AC voltage.

### Excluding the Joule heating effect

In Fig. 1b, we measured positive and negative sweep  $V$ - $I$  curves with the same sweep rates. These two curves lie on top of each other, indicating that the  $V$ - $I$  curves and associated  $I_{c+}$  and  $I_{c-}$  are not dependent on the two sweep directions. As shown in Fig. 1c, the  $V$ - $I$  is asymmetric and  $I_{c+}$  and  $I_{c-}$  have prominently different values. In general, the Joule heating effect is proportional to the heating time and the  $I_{c+}$  (or  $I_{c-}$ ) obtained in positive and negative sweeps undergo different heating times which can cause different local temperatures in sample. If the asymmetric  $V$ - $I$  was induced by the Joule heating effect, the values of  $I_{c+}$  and  $|I_{c-}|$  would switch for the positive and negative sweeps; i.e. the effect would be sweep direction dependent. However, the  $V$ - $I$  curves of positive and negative

sweeps are the same, strongly indicating that the different  $I_{c+}$  and  $I_{c-}$  obtained indeed are intrinsic to the device rather than induced extrinsically by the Joule heating effect.

**Data availability**

The data that support the findings of this study are available from the corresponding author upon request.

**Acknowledgments:**

We thank Justin Song, Gil-Ho Lee and Yongjian Wang for valuable discussions. **Funding:** M.N.A acknowledges that this research was principally supported by the Alexander von Humboldt Foundation Sofia Kovalevskaja Award, the German Federal Ministry of Education and Research's MINERVA ARCHES Award, and the Max Planck Society. Y.-J.Z. acknowledges Shenzhen Science and Technology Project under grant No. JCYJ20180507182246321. S.S.P.P. acknowledges the European Research Council (ERC) under the European Union's Horizon 2020 research and innovation programme (grant agreement no. 670166), Deutsche Forschungsgemeinschaft (DFG, German Research Foundation)—project number 314790414, and Alexander von Humboldt Foundation in the framework of the Alexander von Humboldt Professorship endowed by the Federal Ministry of Education and Research. T.M. acknowledges the David and Lucile Packard Foundation and the Johns Hopkins University Catalyst Award. E.S.T. acknowledges support of NSF DMR 1555340.

**Author contributions:** H.W. and M.N.A. conceived and designed the study. C.P. grew the samples. H.W. and Y.W. fabricated the devices. H.W., Y.W., and P.K.S. performed the transport measurements. H.W. and Y.W. carried out the data analysis. T.M. and M.N.A. are the Principal Investigators. All authors contributed to the preparation of manuscript.

**Competing interests:** The authors declare that they have no competing interests.

**Additional information**

**Correspondence and requests for materials** should be addressed to H.W. and M.N.A.

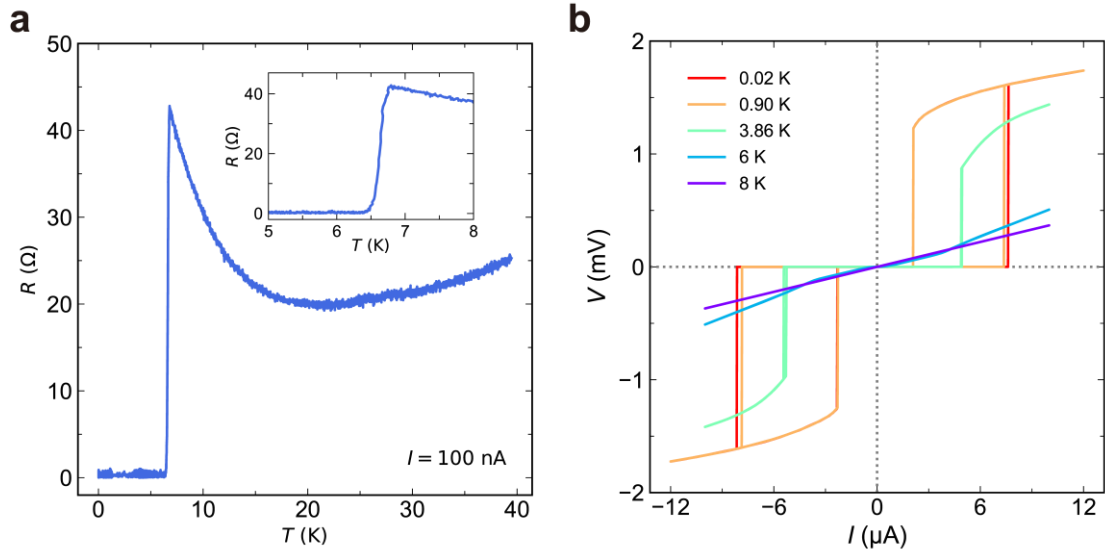


**Fig. S1 | Temperature dependent resistance and  $V$ - $I$  curves of the Josephson diode. a,** Resistance vs. temperature measured using an AC current of 100 nA. Inset shows the enlarged plot near the superconducting transition of 6.6 K. **b,**  $V$ - $I$  curves with positive sweep measured at different temperatures showing nonlinear behavior appearing below  $T_c$ .



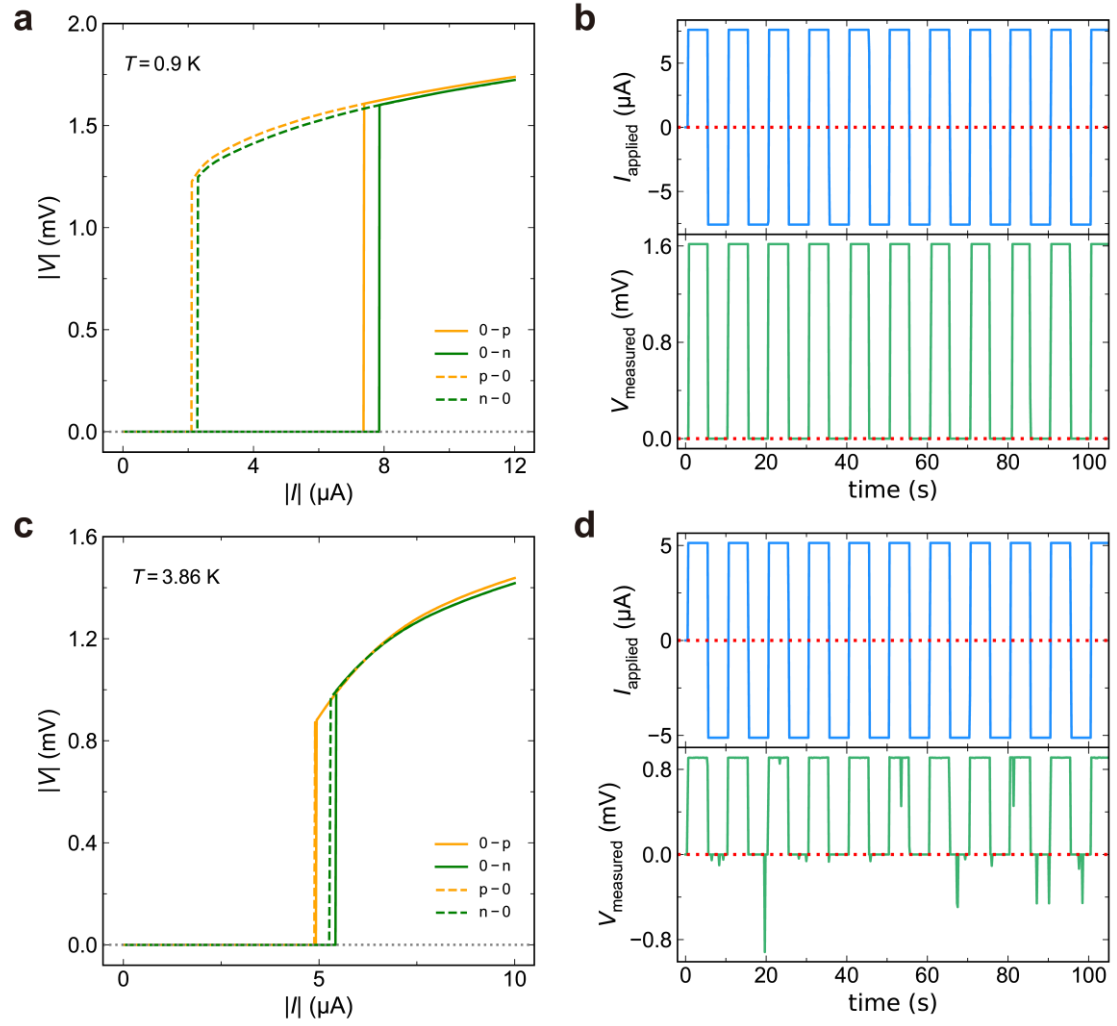


**Fig. S2 |  $V$ - $I$  curves and half-wave rectification at different temperatures.** **a**, Positive sweep  $V$ - $I$  curve measured at 0.9 K. Both  $\Delta I_c$  and  $\Delta I_f$  are visible. **b**, Half-wave rectification measured at 0.9 K with an applied current of 7.6  $\mu$ A at 0.1 Hz. The red dotted lines are the zero lines, showing that junction is in the superconducting state with negative current and switches to the normal state with positive current. **c**, Positive sweep  $V$ - $I$  curve measured at 3.86 K.  $\Delta I_c$  is still visible, while the hysteresis is almost completely suppressed. **d**, Half-wave rectification measured at 3.86 K with an applied current of 5.14  $\mu$ A at 0.1 Hz. The red dotted lines are the zero lines. Imperfect rectification is evident with some punch through error, likely due to thermal fluctuation.

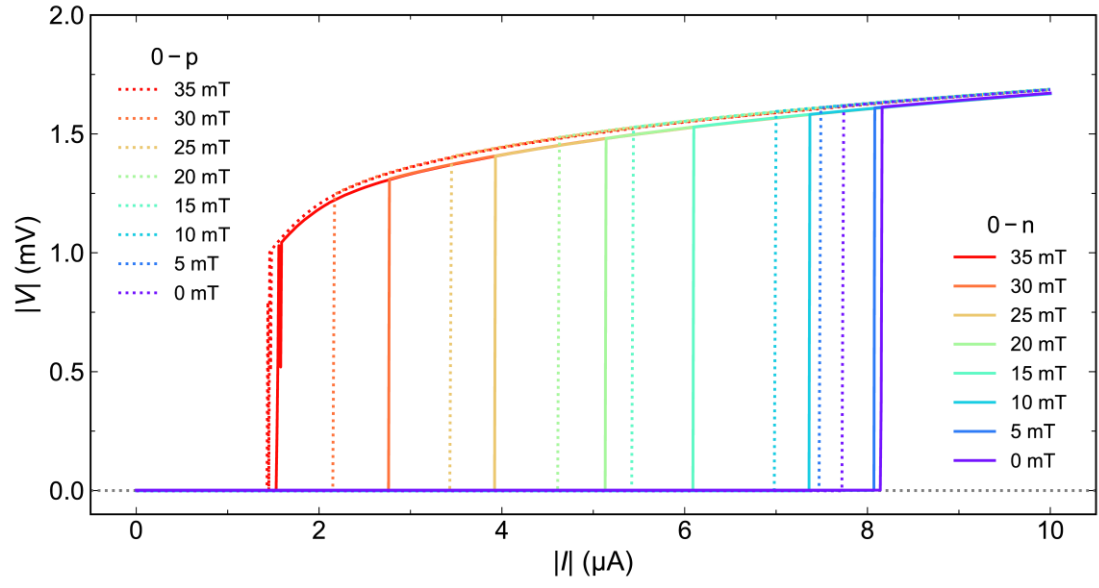


**Fig. S3 |  $V$ - $I$  curves with 0-p and 0-n branches measured at different magnetic fields.** Solid lines are 0-n branches (where  $I_{c-}$  was extracted) and dotted lines are 0-p branches (where  $I_{c+}$  was extracted) corresponding to Fig. 3.  $\Delta I_c$  almost “turns off” at 35 mT.

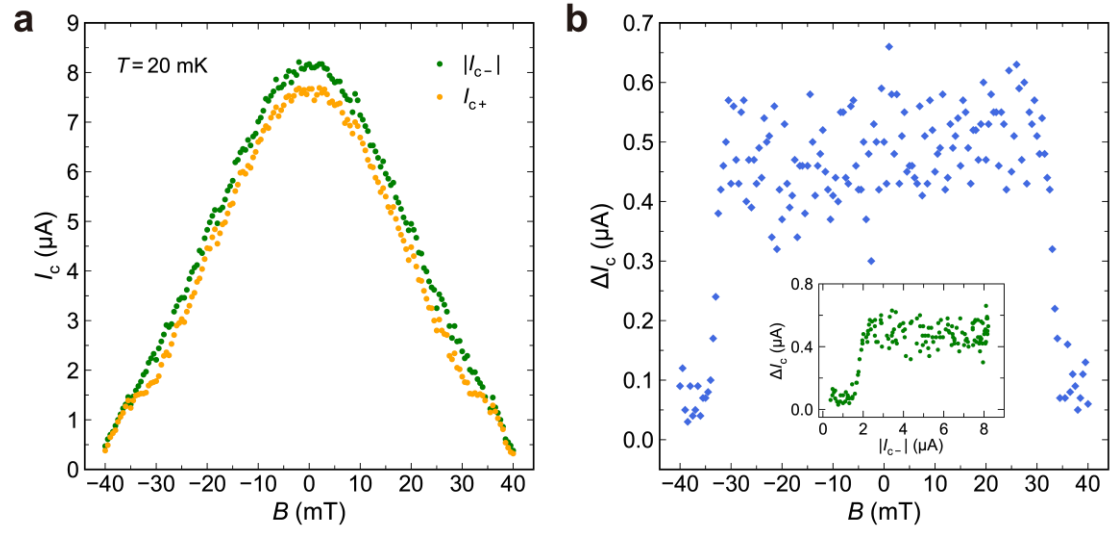


**Fig. S4 | Sweep-up magnetic field dependence of  $I_c$  and  $\Delta I_c$ .** **a**,  $I_{c+}$  (orange dots) and  $|I_{c-}|$  (green dots) obtained from the 0-p and 0-n branches of the positive sweep as a function of applied magnetic field. The in-plane magnetic field was swept from negative to positive. **b**,  $\Delta I_c$  as a function of magnetic field. Inset shows  $\Delta I_c$  as a function of  $|I_{c-}|$  from modulation of magnetic field with the diode effect “turning off” below 2.1  $\mu\text{A}$ . These sweep-up results are nearly identical with the sweep-down results shown in the main text Fig. 3.